



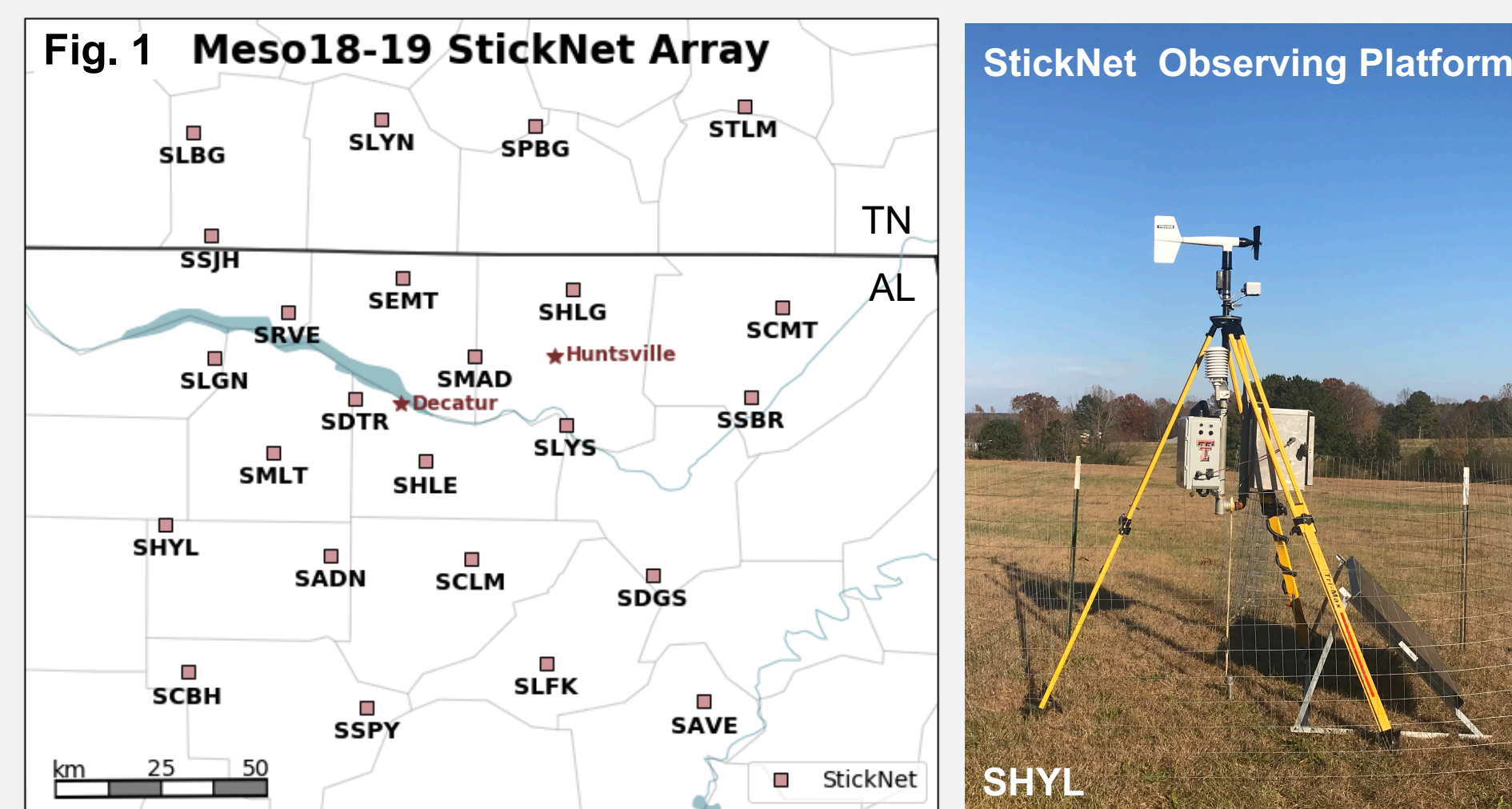
Properties of Cold Pools Observed during the VORTEX-SE Meso18–19 Field Campaign

Jessica M. McDonald¹, Christopher C. Weiss¹, and Aaron J. Hill²

¹Department of Geosciences, Texas Tech University, ²Department of Atmospheric Science, Colorado State University

1. Introduction

Baroclinic regions within supercells and their relationship to tornadogenesis have been a focus of past observational studies. To gather observations of supercells that develop during the Southeast cold season, 24 TTU StickNets (Weiss and Schroeder 2008) were deployed in an array across S TN and N AL (Fig. 1) from Nov 2018 to May 2019. The Meso18-19 dataset builds upon data collected in 2016 and 2017 as part of V-SE.



2. Methods

Observations of supercells that produced inferred vorticity $> 0.003 \text{ s}^{-1}$ or a tornado within 15 km of a StickNet were included in this analysis.

- Data:** Convert 1-Hz data from time to distance using storm motion estimated from radar.
- Base State:** Average thermodynamic variables between 15 and 20 km ahead of cold pool edge (away from forward-flank influences).
- Perturbations:** Find minimum value within 25 km of cold-pool edge and subtract base state from that value.

Calculated thermodynamic variables:

θ_v : estimate of air density including water vapor but not liquid water content.

θ_e : potential buoyancy; a higher value results in larger integrated CAPE. Heavily dependent on moisture content.

Events Meeting Criteria

Meso18-19	Tornadic	# Obs
20190309	No	1
20190314	Yes	3
2016-17	Tornadic	# Obs
20160331	No	7
20160430	No	1
20170301	No	3
20170422	Yes	4

Table 1

3. 14 March 2019 Case Study

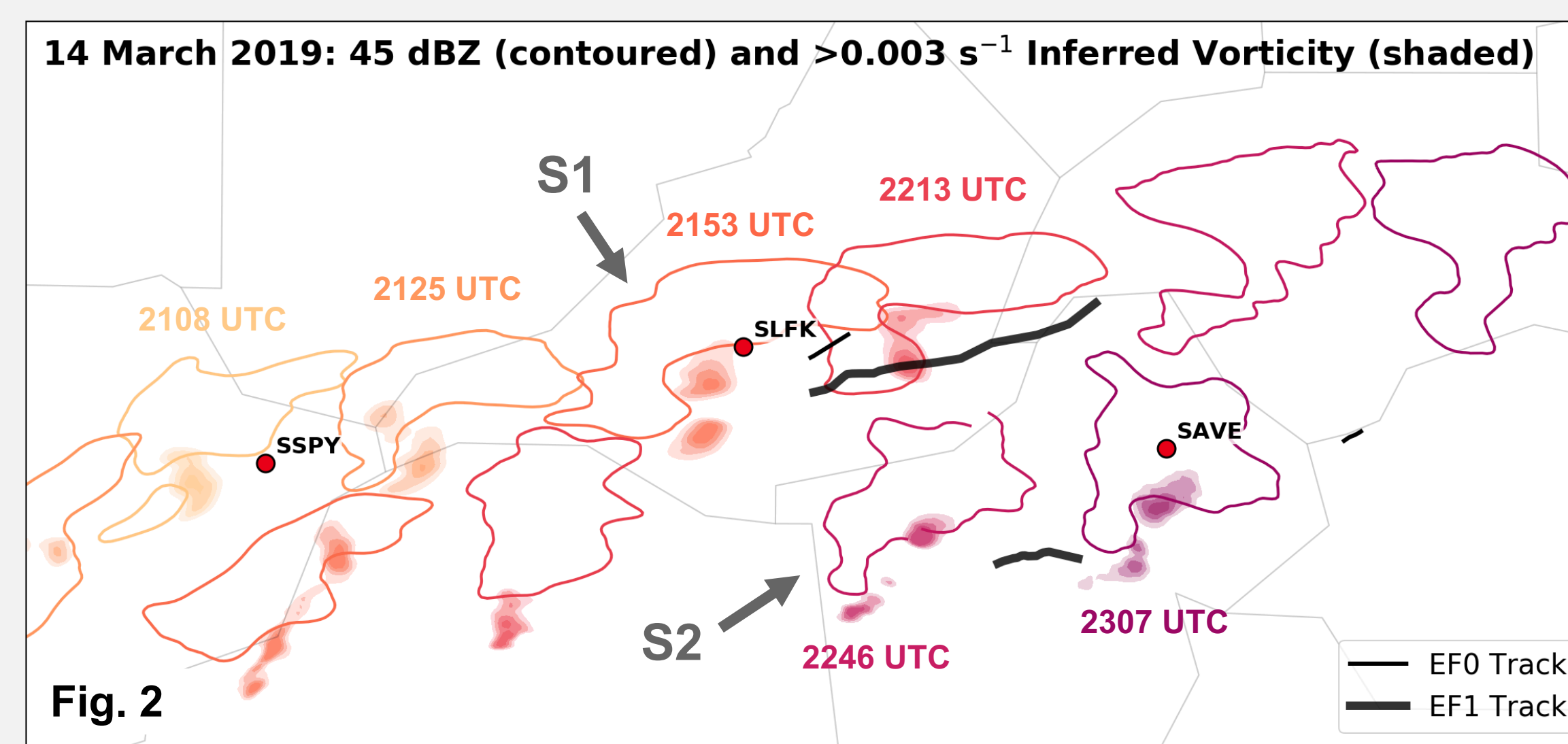


Fig. 2

Two supercells (S1 and S2) impacted three StickNets and produced four tornadoes (Fig. 2). During tornadic stages, both supercells show two distinct thermodynamic regions, labeled R1 and R2 (Figs. 4 and 6). The nontornadic phase of S1 (at SSPY) has less distinct regions.

Estimated Baroclinity

	R1 (K km^{-1})	R2 (K km^{-1})
S1, SSPY (nontornadic)	-0.15	-0.35
S1, SLFK (tornadic)	-0.40	-0.48
S2, SAVE (tornadic)	-0.31	-0.38

Table 2

Northern Supercell (S1)

SSPY – Nontornadic phase. Small deficits and weak baroclinity present (Table 2).

SLFK – Tornadic phase. Strong “inflow low” in P' field, consistent with past observations of a strongly tornadic supercell (Weiss et al. 2015). R1 presents an ideal scenario for baroclinic vorticity generation and stretching: θ'_v is negative and decreasing while θ'_e is positive (Skinner et al. 2011). The baroclinity in both R1 and R2 (Table 2) is stronger than that observed at SSPY.

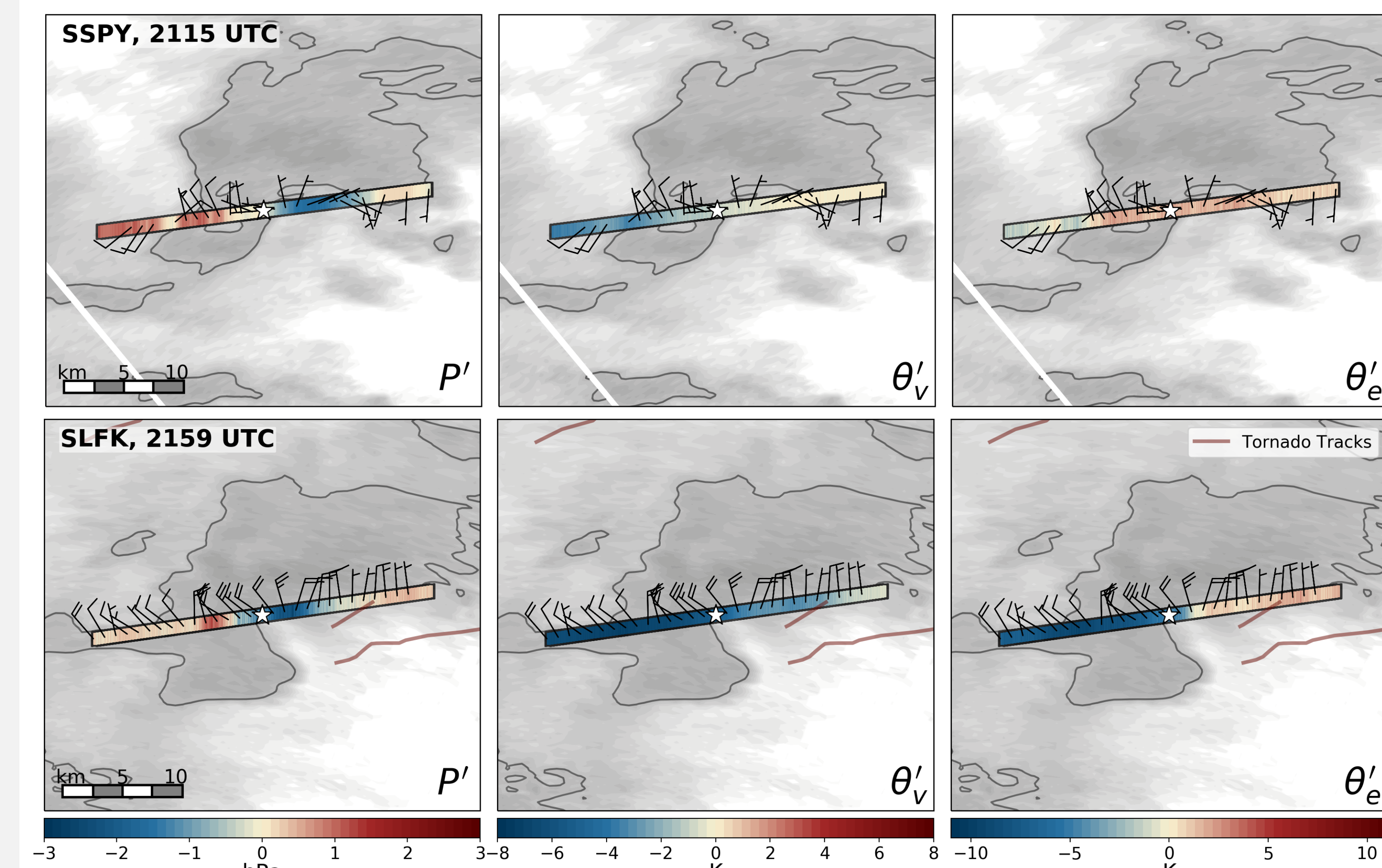


Fig. 3. 1800 s duration time-to-space conversion of thermodynamic variables, plotted at 1 Hz. Wind barbs (ground relative) are averaged and plotted every 60 s. Data are centered in time on the white star. KBMX reflectivity is shaded in gray, and the solid gray contour is 40 dBZ.

Southern Supercell (S2)

SAVE – Tornadic phase. S2 has very similar thermodynamic characteristics as recorded by SLFK, although it is located further into the forward flank than SSPY or SLFK. It has the largest positive pressure perturbations, likely due to hydrostatic effects.

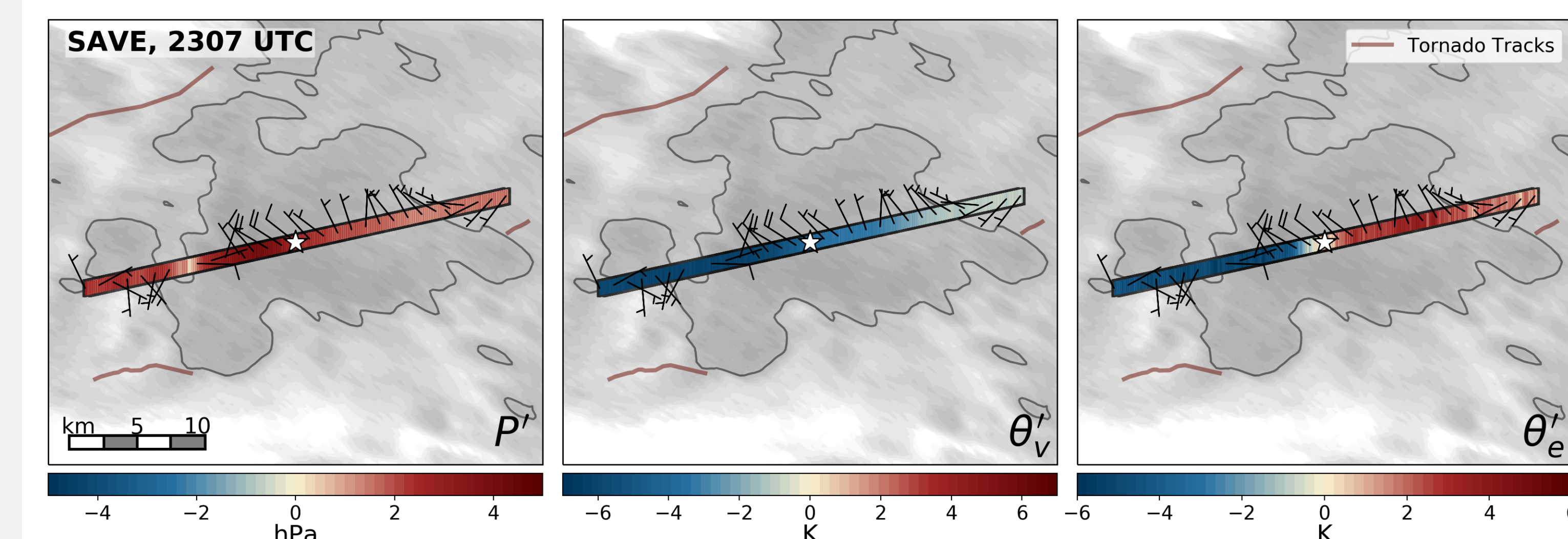


Fig. 5. As in Fig. 3.

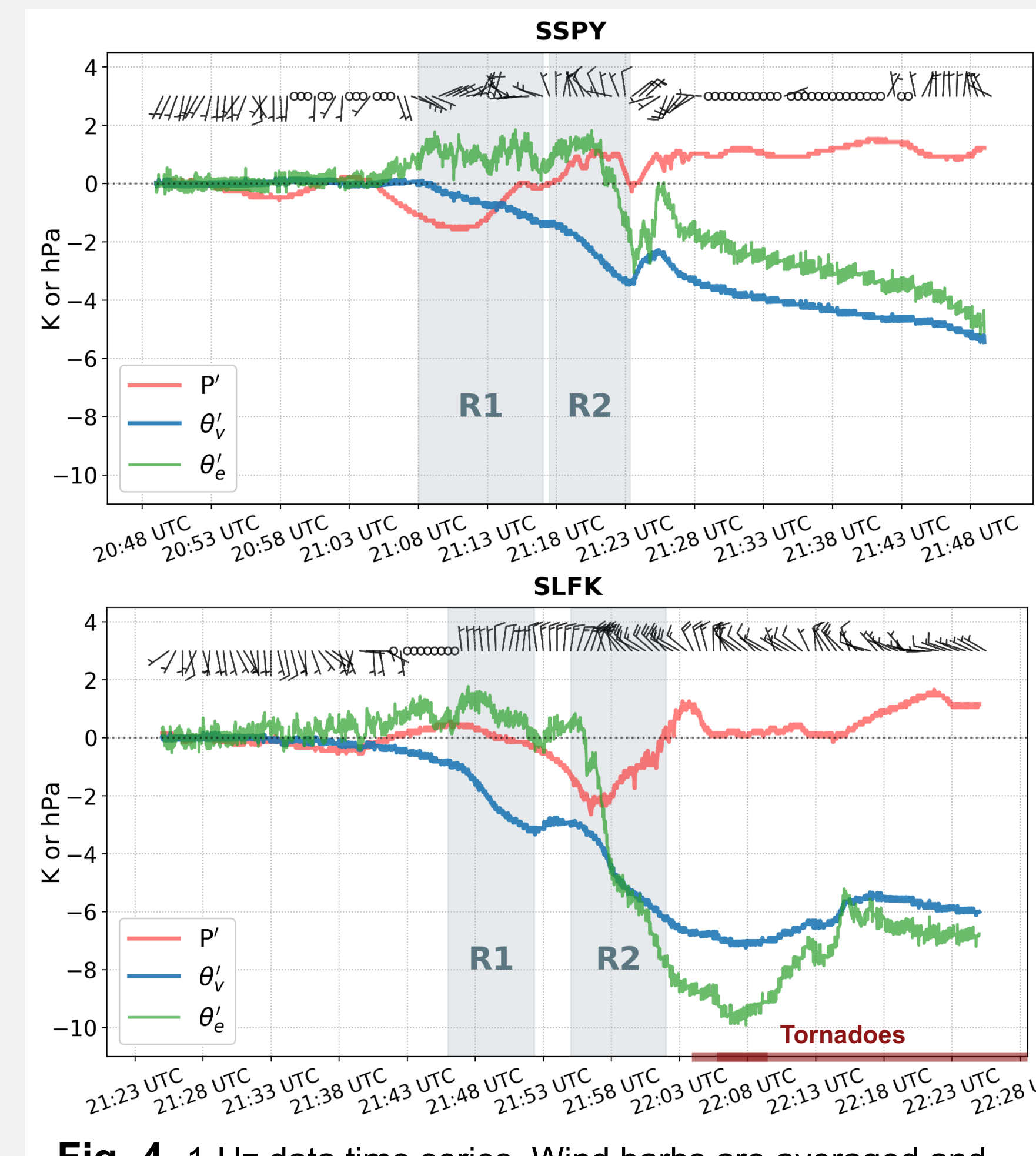


Fig. 4. 1-Hz data time series. Wind barbs are averaged and plotted every 30 s. The solid maroon bars along the x-axis show tornado durations. The solid gray shading highlights the R1 and R2 times over which baroclinity was measured in Table 2.

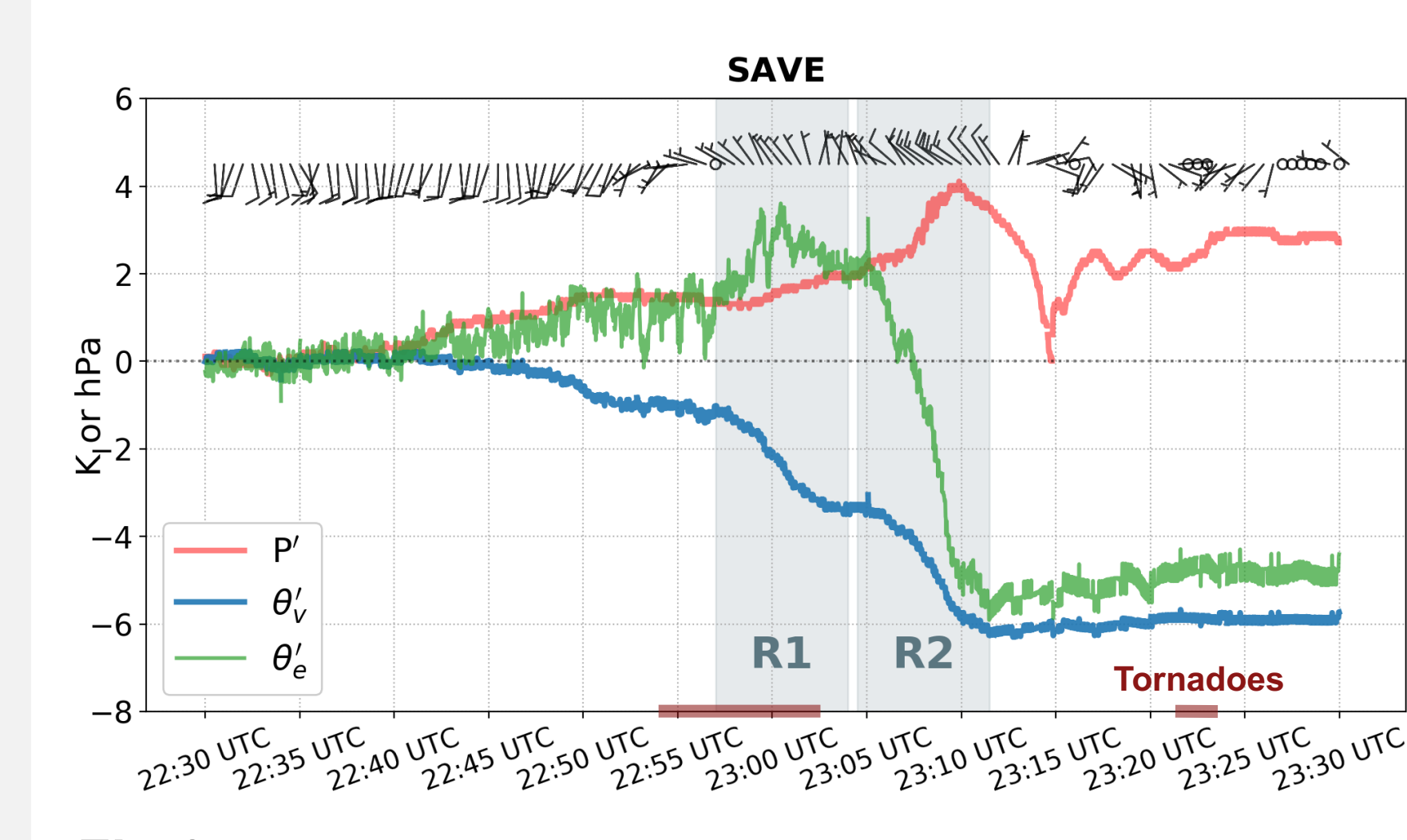


Fig. 6. As in Fig. 4.

4. Meso18-19 and 2016-17

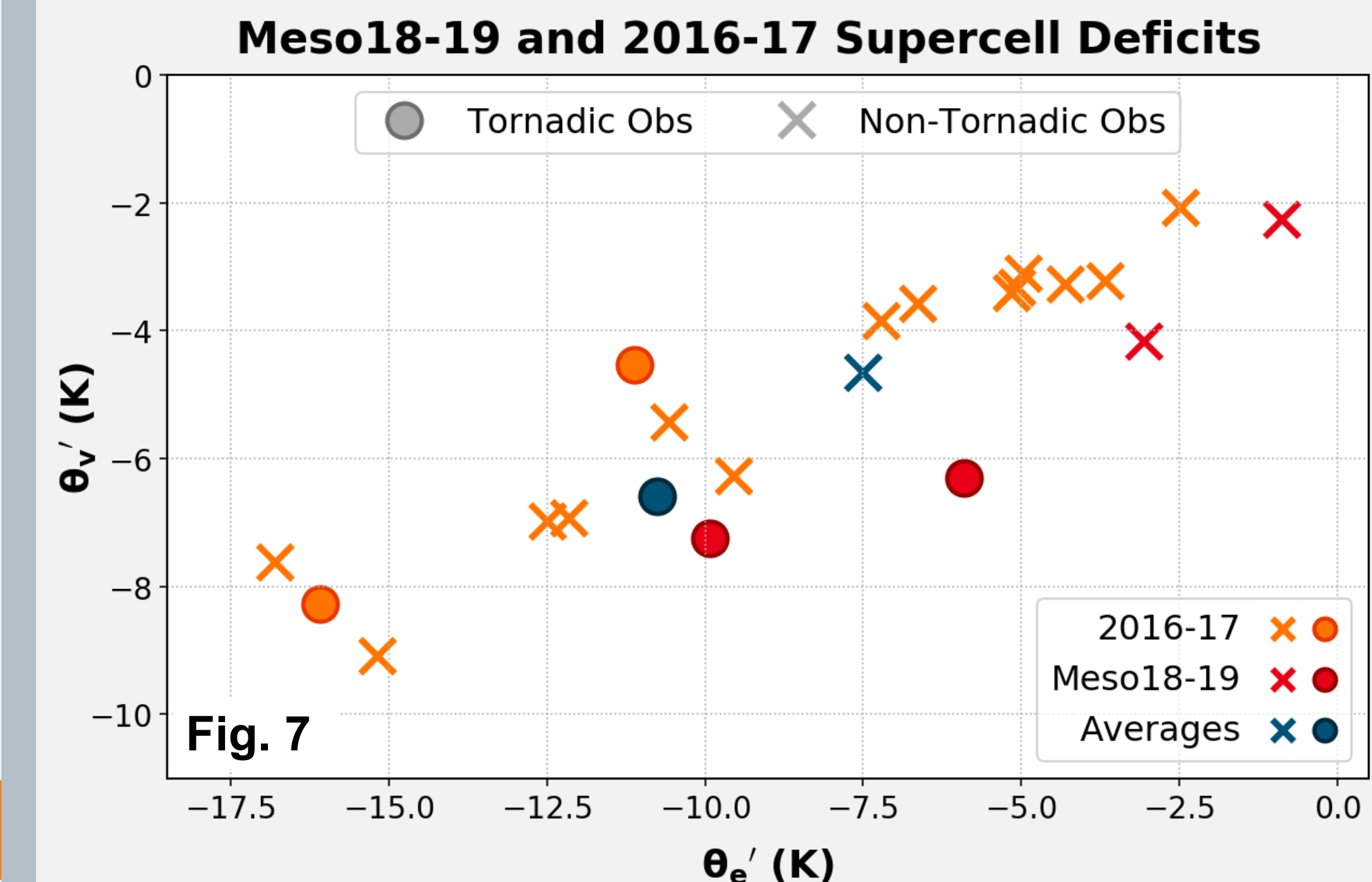


Fig. 7

Average tornadic supercell deficits from 2016-17 and Meso18-19 have greater magnitudes than nontornadic observations (Fig. 7).

Past research found the opposite for strongly tornadic supercells (Markowski et al. 2002, Shabbott and Markowski 2006, Weiss et al. 2015); however, all V-SE observed tornadoes were weak ($\leq \text{EF1}$).

5. Summary

A tornadic supercell had weaker deficits during a nontornadic phase than immediately before tornadogenesis.

- **The stronger baroclinity evident before tornadogenesis may have helped produce more horizontal vorticity.**

Two tornadic supercells presented two baroclinic regions within the forward flank, R1 and R2.

- **R1 had ideal thermodynamic characteristics for producing baroclinic vorticity and then stretching it.**

6. References and Acknowledgements

Markowski, P. M., J. M. Straka, and E. N. Rasmussen, 2002: Direct Surface Thermodynamic Observations within the Rear-Flank Downdrafts of Nontornadic and Tornadic Supercells. *Monthly Weather Review*, 130 (7), 1692–1721, doi:10.1175/1520-0493(2002)130<1692:DSTOWT2.0.CO;2.

Shabbott, C. J., 615 and P. M. Markowski, 2006: Surface In Situ Observations within the Outflow of Forward-Flank Downdrafts of Supercell Thunderstorms. *Monthly Weather Review*, 134, 1422–1441, doi:10.1175/MWR3131.1.

Skinner, P. S., C. C. Weiss, J. L. Schroeder, L. J. Wicker, and M. I. Biggerstaff, 2011: Observations of the Surface Boundary Structure within the 23 May 2007 Perryton, Texas, Supercell. *Mon. Wea. Rev.*, 139 (12), 3730–3749, doi:10.1175/MWR-D-10-05078.1.

Weiss, C. C., and J. L. Schroeder, 2008: StickNet—A new portable, rapidly-deployable, surface observing system. Preprints, 25th Int. Conf. on Interactive Information Processing Systems for Meteorology, Oceanography, and Hydrology, New Orleans, LA, Amer. Meteor. Soc., P4A.1.

Weiss, C. C., D. C. Dowell, J. L. Schroeder, P. S. Skinner, A. E. Reinhart, P. M. Markowski, and Y. P. Richardson, 2015: A Comparison of Near-Surface Buoyancy and Baroclinity across Three VORTEX2 Supercell Intercepts. *Monthly Weather Review*, 143 (7), 2736–2753, doi:10.1175/MWR-D-14-00307.1.

Special thanks to Alex Schueth for providing code to calculate the vorticity fields in Fig. 2 and Abby Hutson for helping improve this poster.

Funding for this project provided by NOAA grants NA17OAR4590206 and NA18OAR4590318